batteries

MDPI

Article

Investigations of Dongyue Series Perfluorosulfonic Acid Membranes for Applications in Proton Exchange Membrane Fuel Cells (PEMFCs)

Ge Meng [1], Xiang Li [2], Mengjie Liu [1,3], Sergey A. Grigoriev [4,5,6,7], Ivan Tolj [8], Jiaqi Shen [1], Chaonan Yue [1] and Chuanyu Sun [1,3,*]

1 School of Electrical Engineering and Automation, Harbin Institute of Technology, Harbin 150001, China; mengge@stu.hit.edu.cn (G.M.)
2 Department of Applied Chemistry, School of Chemistry and Chemical Engineering, Harbin Institute of Technology, Harbin 150001, China
3 Suzhou Research Institute, Harbin Institute of Technology, Suzhou 215104, China
4 Department of Chemistry and Electrochemical Energy, National Research University "Moscow Power Engineering Institute", 14, Krasnokazarmennaya St., Moscow 111250, Russia; grigoryevsa@mpei.ru
5 Department of Electrochemical and Hydrogen Technologies, National Research Centre "Kurchatov Institute", 1, Akademika Kurchatova Sq., Moscow 123182, Russia
6 HySA Infrastructure Center of Competence, Faculty of Engineering, North-West University, Potchefstroom 2531, South Africa
7 Laboratory for Aliphatic Organoboron Compounds, A.N. Nesmeyanov Institute of Organoelement Compounds, Russian Academy of Sciences, 28-1, Vavilova St., Moscow 119334, Russia
8 Faculty of Electrical Engineering, Mechanical Engineering, and Naval Architecture, University of Split, 21000 Split, Croatia; itolj@fesb.hr
* Correspondence: chuanyu.sun@hit.edu.cn

Abstract

This study systematically investigated the physicochemical properties and proton exchange membrane fuel cell (PEMFC) performance of perfluorosulfonic acid (PFSA) membranes with different thicknesses, which were prepared based on the resins produced by Dongyue (China) in comparison with commercial Nafion membranes. It was found that the water uptake of Dongyue membranes is significantly higher than that of Nafion, showing a significant upward trend with the thickness increase. The ion exchange capacity (IEC) of these membranes is ca. 1 mmol·g^{-1}. Moreover, the tensile strength of the Dongyue membrane was positively correlated with the thickness and was significantly higher than that of recast Nafion. Under 80 °C, all Dongyue membranes with various thicknesses (15~45 μm) exhibited PEMFC single-cell performance superior to that of Nafion. The maximum power density is observed with a thickness of 25 μm, reaching 851.76 mW·cm^{-2}, which is higher than that of Nafion (635.99 mW·cm^{-2}). However, the oxidative stability of the prepared Dongyue PFSA series membranes exhibits a slight deficit compared to commercial Nafion membranes. Subsequently, the modification and optimization of preparation processes can be employed to improve the mechanical and chemical stability of Dongyue PFSA membranes.

Keywords: perfluorosulfonic acid (PFSA) membrane; proton exchange membrane fuel cell (PEMFC); hydrogen energy system; Nafion; Dongyue; membrane thickness; power density; proton conductivity; ion exchange capacity; oxidative stability

Academic Editors: Mingtao Li, Piercarlo Mustarelli and Manickam Minakshi

Received: 18 June 2025
Revised: 4 July 2025
Accepted: 17 July 2025
Published: 20 July 2025

Citation: Meng, G.; Li, X.; Liu, M.; Grigoriev, S.A.; Tolj, I.; Shen, J.; Yue, C.; Sun, C. Investigations of Dongyue Series Perfluorosulfonic Acid Membranes for Applications in Proton Exchange Membrane Fuel Cells (PEMFCs). *Batteries* **2025**, *11*, 277. https://doi.org/10.3390/batteries11070277

1. Introduction

During human development progress, there is an inseparable link between economic development and energy consumption. Since the Industrial Revolution, human demand for energy has continued to grow. In addition, traditional fossil fuels have limited reserves and are unsustainable, which cause serious environmental pollution [1,2]. With the continuous depletion of traditional fossil fuel reserves and the high attention to their impact on the environment, the development of renewable energy, such as solar energy and hydrogen energy, has become a research hotspot. Among them, hydrogen energy has made major breakthroughs after long-term development. Hydrogen production through surplus electricity electrolysis of water is one of the main methods to obtain green hydrogen. It has great potential in the transformation to clean energy, and can also effectively solve the volatility and intermittency problems of renewable energy sources [3]. Therefore, fuel cells, such as hydrogen to energy conversion devices, have attracted widespread attention from researchers around the world due to their exceptional power density, low thermal operation requirements, and zero environmental pollution.

Fuel cells, also known as electrochemical power generators, can directly transform the chemical energy of fuel into electricity without combustion, thus breaking away from the limitations of the Carnot cycle and achieving higher power generation efficiency [4]. In theory, its energy conversion efficiency can reach over 85%, and in practical work, it is about 40 to 60% [5]. It has great potential in various applications, such as large-scale power plants, portable power sources, automotive batteries, etc. [6,7], and the most common fuel is hydrogen. Among them, proton exchange membrane fuel cells (PEMFCs) have the advantage of high efficiency, cleanliness, and wide temperature adaptability. They have the widest application range, have been comprehensively investigated, and are the most promising candidates in future transportation electrification. However, their shortcomings, such as poor durability and high cost, need to be addressed urgently [8–10]. Proton exchange membrane (PEM) is the core material of PEMFCs, which plays a decisive role in the operating conditions and output performance. Its main function in fuel cells is to isolate oxidants in the cathode and reduce agents in the anode while simultaneously conducting cations [11,12].

At present, perfluorosulfonic acid membrane (PFSA) is the most widely used and best-performing PEM in the current PEMFC market. Its hydrophobic fluorinated main chain and hydrophilic sulfonic acid side chain give it the advantages of high proton conductivity when the membrane is hydrated, due to the significant phase separation between the hydrophobic backbones and hydrophilic clusters, which provides the pathways for proton conduction. Meanwhile, the PFSA membranes also possess high mechanical strength and high antioxidant stability. Conventional and commercial PFSA membranes on the market include Flemion® produced by Asahi Glass (Tokyo, Japan), Aciplex-S® produced by Asahi Chemical (Osaka, Japan), etc. Among them, the Nafion® membranes produced by DuPont (Wilmington, DE, USA) are still considered the standard benchmark membrane for PEMFCs [4]. Jennifer et al. [13] reported that the conductivity of Nafion 211 PEM with a thickness of 25 μm reached 0.13 S/cm at 80 °C and RH = 95%. However, the complex fabrication procedures and high cost hinder their further application in industries.

In order to reduce the cost of PEMs, researchers are actively seeking low-cost alternatives to Nafion, such as sulfonated polyethylene ether ketone (SPEEK). Erce et al. [14] studied the effect of SPEEK on the performance of proton exchange membranes, and Teixeira et al. [15] researched a new type of modified SPEEK membrane. Sun et al. [16] studied the properties and battery efficiency of WO_3-doped modified SPEEK membranes. But its conductivity and hydrothermal stability need to be improved and are not as good as perfluorosulfonic acid membranes. This article selected PFSA resin dispersion produced in

Dongyue, Shandong, China, which is priced at USD 500 per liter. To prepare a 10 × 10 cm membrane sample with a thickness of 25 μm, approximately 10 mL of PFSA resin dispersion is used, which is about USD 5. In addition, the cost of other experimental consumables is less than USD 5. The price of a 10 × 10 cm Nafion membrane with the same thickness of 25 μm is USD 30, much higher than that of Dongyue PFSA membranes.

Meanwhile, reducing the thickness of PEM can also reduce the preparation cost and promote further large-scale and commercial applications of PFSA membranes. The thickness of PEM belongs to its own physical characteristics and affects the comprehensive performance of PEMs [17]. Studies have shown that the conductivity of PEM is almost linearly related to the membrane thickness [18–20]. The thicker the PEM, the higher the resistance during ion conduction, as well as the higher the ohmic loss of the PEMFC, which restricts the maximum power density and reduces PEMFC performance [21,22]. Therefore, diminishing the thickness of PEM is one of the solutions to improve PEMFC performance. In addition, it can be beneficial to increase the hydration rate, enhance the proton conductivity, and further promote the output performance [4]. With the decrease in the PEM thickness, its mechanical properties may deteriorate, and the membrane can be easily crushed and punctured, which leads to safety challenges for PEMFC operation. Therefore, the degree of reduction in membrane thickness should be accurately regulated and cannot be limitless. The mechanical properties of the membrane can be improved through modification and other approaches, so it is necessary to comprehensively consider the various physical and chemical properties of the PEM and finally select the optimal thickness for the PEM.

To strengthen the mechanical stability of PEMs, Yin et al. [23] synthesized multiple inorganic–organic hybrid membranes including Nafion as the polymer matrix and TiO_2/SiO_2 nanofillers as the inorganic components, and the PEMFC assembled with those hybrid membranes was characterized. The results indicated that the composite membrane exhibited a denser structure and the breaking strength of the membrane was enhanced. Di Noto et al. [24] prepared $[(ZrO_2)\cdot(HfO_2)_{0.25}]$, $[(SiO_2)\cdot(HfO_2)_{0.28}]$ and Nafion hybrid membranes and studied their conductivity mechanism. Vittadello et al. [25] prepared [Nafion/(HfO_2)n] hybrid membranes with better performance and elucidated the conduction mechanism of the composite membranes. Vinothkannan et al. [26] added CeO_2-TiC inorganic fillers into the Nafion matrix and prepared the hybrid membranes by solution casting methods for modification. The results demonstrated that the thermal stability of the hybrid PEM increased by 1.4 times and the tensile strength increased by 1.3 times compared to the pristine Nafion membrane. The above results all reveal that the addition of inorganic fillers can effectively improve the mechanical strength of pristine PEM. Sun [27] prepared a [Nafion/(WO_3)x] hybrid membrane, which showed higher energy efficiency and coulombic efficiency, and improved the performance of the proton exchange membrane. Li et al. [9] prepared Nafion/PVDF composite membranes by blending PVDF polymer with Nafion resin. The results showed that the mechanical strength of the blend membrane markedly surpassed that of the Nafion 212 membrane, with a 48.0% increase in breaking strength and a 100% increase in breaking elongation. The resistance to dimensional change in the blend membrane was also enhanced. In addition, by incorporating sulfonating and fluorinating polyetheretherketone components, the physical–chemical properties of the PEM can also be comprehensively improved, including the enhancement in proton conductivity and mechanical properties.

In this work, a series of PFSA membranes with different thicknesses (15~55 μm) were prepared using a lower-cost PFSA resin produced by Dongyue. Their physical and chemical properties, such as water uptake, swelling ratio, proton conductivity, and mechanical and antioxidant stability, were measured, and their performance was further evaluated through

PEMFC single-cell tests. The test results of the membrane samples with different thicknesses were compared with each other and with the commercial PFSA membrane Nafion as a benchmark. It was found that the proton conductivity, water uptake, and swelling ratio of the Dongyue PFSA membrane were higher than those of the Nafion membrane. Most importantly, the maximum power density of its PEMFC single-cell test was also higher than that of the Nafion membrane, showing good cell performance. But its antioxidant property was slightly inferior to that of the Nafion membrane, and its antioxidant property could be enhanced by subsequent modification and other means. Through this experiment, the optimal membrane thickness of the Dongyue PFSA membrane in PEMFC operation was determined, which will help reduce the cost of fuel cell proton exchange membranes and further accelerate the commercialization of the new PFSA membrane series in PEMFC.

2. Materials and Methods

The PFSA resin dispersion (DH2210, polymer content 10.0~11.0%, water content 45 ± 3%, VOC content 45 ± 3%) was purchased from Shandong Dongyue Future Hydrogen Energy Materials Co., Ltd., Zibo, China. The Nafion 211 membrane, the anode gas diffusion electrode with a platinum loading of 0.1 mg/cm^3, and the cathode gas diffusion electrode with a platinum loading of 0.3 mg/cm^3 were purchased from Sinero Technology Co., Ltd., Taicang, China. The N,N-Dimethylformamide (DMF) solution was of analytical grade and purchased from Sinopharm Chemical Reagent Co., Ltd., Shanghai, China. The concentrated H_2SO_4 solution (98%) was of analytical grade and purchased from Xilong Scientific Co., Ltd., Guangzhou, China. The 3% H_2O_2 solution was purchased from Harbin Ruibiao Technology Co., Ltd., Harbin, China. Other chemicals were also of analytical grade.

2.1. Membrane Preparation

First, a batch of different volumes (2~10 mL) of PFSA resin dispersions was placed in multiple beakers, and the solvent components such as water and ethanol in the ionomer solutions were evaporated gradually as the beakers were placed in the 80 °C water bath environment. When all the solvent components were completely removed, the remaining layer at the bottom beaker is the obtained PFSA resin in solid form. Then, an appropriate amount (10 mL is employed in this work) of DMF solvent was added into the corresponding beaker. The obtained mixture in the beaker was heated and stirred with a magnetic stirrer. The beaker was placed in an 80 °C water bath and a glass surface dish was placed on top of the beaker to prevent the DMF solvent inside from evaporating completely. When the PFSA resins are completely dissolved in the DMF solvent, a uniform and clear solution can be obtained. Then, the solution was poured into a 10 cm diameter Petri dish and placed in an 80 °C drying oven for 24 h until the DMF was completely evaporated. Finally, the Petri dish was taken out and deionized water was poured into it to make the PEM swell. At this time, the membrane was automatically separated from the bottom of the Petri dish. The prepared membranes were dried in an oven for 12 h, and then their thicknesses were measured using a spiral micrometer and recorded. Thus, by using perfluorosulfonic acid resin dispersions of different volumes (2, 4, 6, 8, and 10 mL), a series of PFSA membranes with different thicknesses (15, 25, 35, 45, and 55 μm) were obtained, which were named PFSA-15, PFSA-25, PFSA-35, PFSA-45, and PFSA-55.

Then, all the obtained Dongyue PFSA membrane samples were pre-treated by the following steps: (1) The membrane samples were placed in a 3% H_2O_2 solution and heated in an 80 °C water bath for 1 h to remove organic impurities, and then rinsed with deionized water to remove the residual H_2O_2 species. (2) The processed membrane sample after step (1) was further heated and activated at 80 °C for 1 h in the 1M H_2SO_4 aqueous solution, then the sample was rinsed with deionized water until neutral. (3) The obtained sample

was finally heated in deionized water at 80 °C for 30 min to remove all the possible excess impurities. The pre-treated membranes were placed in the sample bags and were labeled for later testing.

2.2. Membrane Characterization

2.2.1. Scanning Electron Microscopy (SEM)

SEM was adopted to acquire the microscopic morphology of the PFSA membrane samples. Before the scanning operation, the samples should be cut into small pieces of 1 × 1 cm and dried in air flow for 24 h. In order to obtain a cross-sectional SEM image of the membrane sample, the membrane sample was completely immersed in liquid nitrogen and rapidly cooled to a brittle state. Then, a tool (tweezers) was used to perform brittle fracture in liquid nitrogen. Then, the treated samples (surface and cross-section) were fixed on the SEM test sample stage with conductive tape. Finally, the sample stage with the membrane sample attached was treated with gold/platinum spray to improve their conductivity. The SU8010 field emission SEM (Hitchi-SU8010, Tokyo, Japan), produced by Hitachi, Ltd., was employed as the SEM instrument to conduct the membrane morphology investigations.

2.2.2. Fourier Transform Infrared (FT-IR) Microspectroscopy

The FT-IR spectra of the prepared Dongyue PFSA membranes were characterized through a FT-IR spectrometer (Zhongke Ruijie Great 20, Tianjin, China), and the characteristic peaks in the FT-IR spectra were analyzed in detail. The membrane samples were dried in a blast drying oven for 12 h to remove physically adsorbed water. The testing wavelength was in between 550 and 4000 cm^{-1} and the testing method adopted the Attenuated Total Reflectance (ATR) mode. Firstly, the pressure rod of Golden Gate (Specac Ltd., Orpington, United Kingdom) is pressed tightly onto the crystal to collect the air background spectrum. Then, the membrane sample is placed directly on the crystal and pressed tightly with the pressure rod to start scanning, obtaining the FT-IR curve of the sample.

2.2.3. Water Uptake (WU) and Swelling Ratio (SR)

The WU and SR of the PEM determine its proton conductivity and internal resistance of the membrane electrode assembly (MEA). To evaluate the WU and SR of the membrane, the PEM sample was first immersed in deionized water at room temperature for 24 h to fully absorb water. Then, the surface moisture was wiped off with filter paper immediately before weighing the sample. In this way, the length, thickness, and weight of PEMs under the wet state were measured. The sample was then dried in an 80 °C oven for 24 h to obtain the dry membrane. And then the length, thickness, and weight of the PEMs under the dry state were measured and recorded. Finally, the WU and SR of the PEM can be derived as follows [28]:

$$\text{Water uptake}(\%) = \frac{W_w - W_d}{W_d} \times 100\% \quad (1)$$

$$\text{Length swelling ratio}(\%) = \frac{L_w - L_d}{L_d} \times 100\% \quad (2)$$

$$\text{Thickness swelling ratio}(\%) = \frac{T_w - T_d}{T_d} \times 100\% \quad (3)$$

where W_w and W_d denote the wet/dry membrane weights, L_w and L_d represent the wet/dry membrane lengths, and T_w and T_d are the thicknesses of the wet and dry membranes, respectively. Three parallel tests for each parameter were performed and the average values were calculated as the final result.

2.2.4. Ion Exchange Capacity (IEC)

The IEC of the membrane was determined via the traditional acid–base titration. The dry membrane was firstly immersed in a saturated NaCl solution for 24 h to fully exchange Na^+ ions in the solution with H^+ ions (protons) from the membrane. Then, phenolphthalein reagent was added to the solution, and the obtained solution was titrated with the 0.01 mol/L NaOH solution. The volume of NaOH solution consumed for the titration was recorded, and the IEC can be determined using the following equation [29]:

$$\mathrm{IEC}\left(\mathrm{mmol}\cdot\mathrm{g}^{-1}\right) = \frac{C_{NaOH} \times N_{NaOH}}{W_d} \tag{4}$$

where V_{NaOH} is the volume of NaOH solution consumed during the acid–base titration, and C_{NaOH} denotes the concentration of the adopted NaOH solution employed.

2.2.5. Proton Conductivity

The PFSA membranes were cut into a square shape with a size of 3 × 3 cm, and each membrane was placed in a test fixture for membrane conductivity (Wuhan Chuxin Technology Co., Ltd., Wuhan, China). The physical and schematic diagrams of the fixture are shown below. The electrochemical workstation (Shanghai Chenhua Instrument Co., Ltd., CHI660E, Shanghai, China) was employed to measure the resistance of the PEM at various temperatures and RH = 100% through electrochemical impedance spectroscopy (EIS). The test fixture was placed in a beaker and heated in a water bath to control different test temperatures of the samples, as shown in Figure 1.

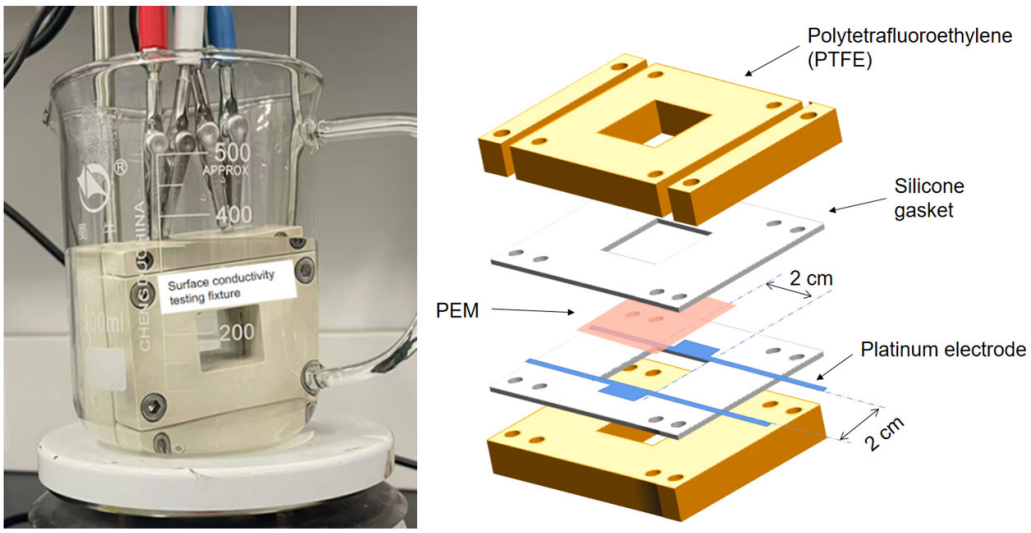

Figure 1. Physical and structural diagrams of proton conductivity testing fixture.

The EIS test frequency ranged from 1 Hz to 10 kHz, and the AC amplitude was 5 mV. After obtaining the EIS curve, the internal resistance of the membrane was obtained by equivalent circuit fitting. The proton conductivity (σ) of the membrane can be calculated according to the following formula:

$$\sigma = \frac{L}{R \times A} \tag{5}$$

where σ is the proton conductivity of the PEM sample, with the unit in S cm^{-1}; L is the distance between the two electrodes, in cm; A is the test area of the PEM, in cm^2; and R is the resistance of the PEM, in Ω. Each parameter was measured repeatedly three times, and the average value was taken as the final result.

2.2.6. Mechanical Properties

PEMs are required to possess a certain mechanical strength to meet the clamping force generated by multiple screws during PEMFC operation. The mechanical strength of the PEM samples was tested using the electronic universal testing machine (SENS, CMT2000 series, Shenzhen, China). The PEMs were firstly cut into 5 × 2 cm strips and clamped into the fixtures, after which the initial distance between the bottom and top of the fixtures and the PEM thickness were recorded. The tensile tests were performed at room temperature at a speed of 50 mm/s to obtain the tensile strength/strain at break and the stress–strain curve of the PEM samples. Each PEM sample was tested three times and the average value was taken.

2.2.7. Thermogravimetric Analysis (TGA)

The thermal stability of the PFSA membranes was characterized by a thermogravimetric synchronous thermal analyzer (Nanjing Dazhan Testing Instrument Co., Ltd., Nanjing, China). The specific steps are as follows: the dried PEM sample was cut into fragments with a weight of ca. 10 mg and then placed in the sample chamber made with ceramics. The sample was heated from room temperature to 750 °C at a temperature rise rate of 10 °C/min in an air atmosphere to obtain the TGA curve of the PEM sample.

2.2.8. Chemical Stability

During the operation of the fuel cell, the product of the two electron reaction of oxygen on the catalyst surface is H_2O_2, which decomposes under the action of metal cations to produce hydroxyl radicals HO· and hydrogen peroxide radicals HOO. The generated free radicals will attack the C-S bonds and C-O bonds in the PFSA polymers, leading to polymer decomposition. The decomposition and loss of sulfonic acid groups in the attacked membrane can lead to a decrease in its proton conductivity. The attack on carbon atoms on the main and side chains can lead to chemical degradation and thinning of the PFSA membranes, resulting in cracks, punctures, pinholes, etc. The degraded membrane material may cause hydrogen and oxygen mixing, local hot spots (dead zones), etc., which seriously reduce the output performance of PEMFCs. Therefore, the durability of PEM and its prepared MEA is a key indicator of fuel cells. The abundant HO in Fenton solution can simulate the free radical environment during PEMFC operation, making it the primary approach for determining the chemical stability and durability of PEMs [19,20]. Firstly, the PEM samples with different thicknesses were cut into a square shape with a size of 3 × 3 cm, and then the initial dry weight and proton conductivity (50 °C, RH = 100%) of the membranes were measured, respectively. Subsequently, the PEM samples were immersed in Fenton solution (3% H_2O_2 + 10 ppm Fe^{2+}) at 80 °C for 24 h, after which the sample was removed and washed several times with deionized water. Then, the proton conductivity of all tested membranes with multiple thicknesses was measured under identical conditions. Finally, the PEM samples were dried at 60 °C for more than 12 h, and the final weight of the dried membranes was measured. FT-IR testing was conducted on the membrane after the Fenton oxidation experiment to analyze the changes in functional groups in the membrane after oxidation.

2.3. PEMFC Single-Cell Performance

The PEMFC single-cell is mainly composed of bipolar plates and MEA, and MEA typically includes gas diffusion layers, PEM, and catalysts [30]. For the fabrication of MEAs, the PEM sample was cut into a square shape with a size of 3.5 × 3.5 cm. The MEA is stacked from top to bottom in the order of anode gas diffusion layer (GDL), anode catalyst, PEM, cathode catalyst, and cathode GDL. The gas diffusion electrode (GDE) was purchased

from Suzhou Shengernuo Co., Ltd., Suzhou, China; the platinum loading of the anode was 0.1 mg/cm^2 and the platinum loading of the cathode was 0.3 mg/cm^2. The carbon paper used is 235 μm thick carbon paper from Japan Toray. For the assembling process of MEA, the stacked components were hot-pressed together at 115 °C and 0.3 MPa for 5 min by hot press (DRK223, Shandong Derui Instrument Co., Ltd., Weifang, China). The PEMFC single-cell was assembled with endplates, bipolar plates with flow channels, and the MEA. The size of a single cell is 10 × 10 cm, and the active area of the MEA is 5 cm^2. Eight screws and a torque wrench were used to adjust the clamping force of 6 N to tighten the single-cell, fix various components such as MEA, and ensure that the single-cell did not leak. And 4 thermocouples were inserted into the single-cell for constant temperature control. The assembled single-cell is shown in Figure 2.

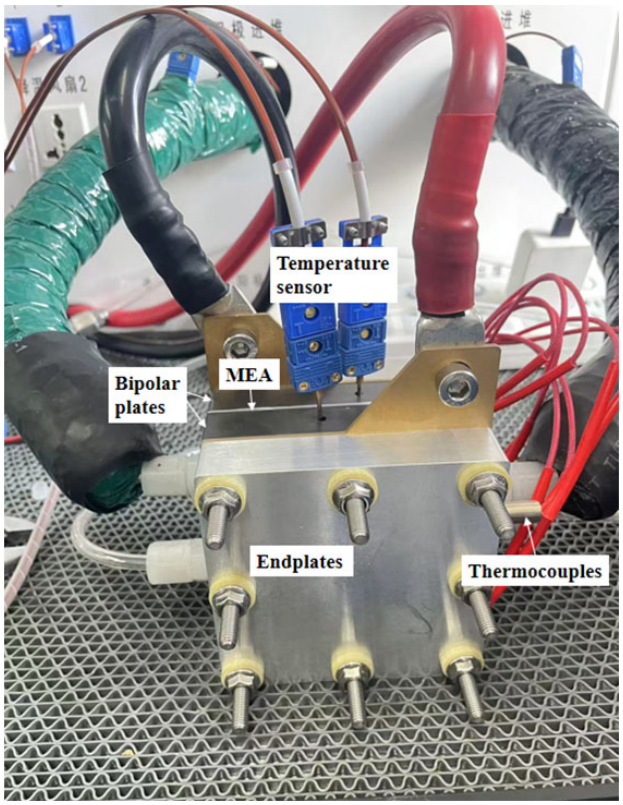

Figure 2. Assembled single-cell for testing.

The polarization curve of the PEMFC single-cell assembled with the above-mentioned MEAs was measured by a YK-A10 PEMFC test bench (Dalian Yuke Innovation Technology Co., Ltd., Dalian, China). The hydrogen used for battery testing is supplied by a high-pressure hydrogen bottle, and the air is supplied by an air compressor. Before performance tests, the MEA is activated by a 0.11 V constant voltage for at least 30 min. The working dew point temperature of the PEMFC single-cell for test conditions was set to 80 °C (100% relative humidity), and hydrogen and air were injected into the anode and cathode, respectively, with the flow rates kept at 300 and 700 mL/min, respectively. The two-stage back pressure was set to 1 MPa and kept constant. The test uses the constant current method. The current test starts from 0 A and increases by 0.1 A. When the peak power density is reached and then continues to decrease, the test is stopped. The PEMFC single-cell test bench is shown in Figure 3.

Figure 3. The PEMFC single-cell test bench.

3. Results and Discussion

3.1. Morphology of PFSA Membranes

The surface morphology of the Dongyue PFSA series membranes is characterized by the SEM and all membrane images exhibit the same characteristics. The morphological images of PFSA-25 at different magnifications are shown in Figure 4 as a representative. The SEM images reveal that the novel PFSA series membranes exhibit a dense, smooth, and uniform surface structure, with no insoluble components or particles on the surface. Moreover, there are no obvious wrinkles, pores, or defects. This is consistent with the SEM images of Nafion membranes or other PFSA membranes in the literature [31].

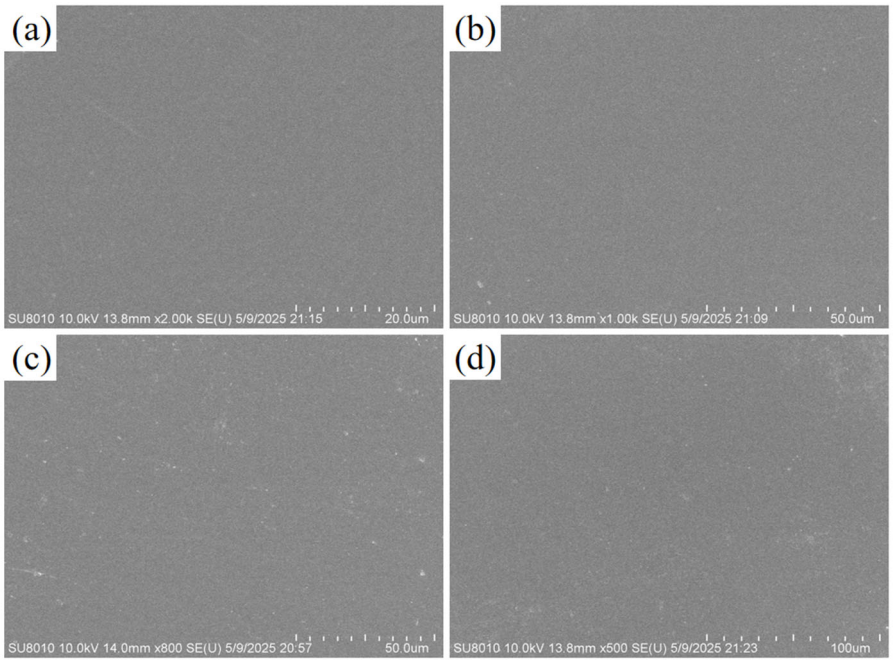

Figure 4. High-resolution SEM images of the surface of the PFSA-25 membrane at different magnifications. (**a**) ×2000 magnification SEM view; (**b**) ×1000 magnification SEM view; (**c**) ×800 magnification SEM view; (**d**) ×500 magnification SEM view.

All cross-sectional SEM images of the membrane showed consistent performance, and Figure 5 shows the cross-section SEM images of PFSA-25 magnified 3000 and 5000 times, respectively. From the image, it can be seen that the PFSA membrane has a uniform thickness, with no pores or cracks at high magnification, and no foreign particles or impurities blocking the proton channel. The thickness of the PFSA-25 membrane was measured to be 23–27 μm using a micrometer after drying in a drying oven at 80 °C for 12 h. However, the SEM cross-section of the membrane sample after water absorption at room temperature (calculated according to the scale bar) showed that the thickness was about 28 μm. This difference is consistent with the expectation of membrane swelling due to water absorption, indicating that the thickness measurement results of the PFSA-25 membrane are consistent. Similar phenomena were observed for other membrane samples.

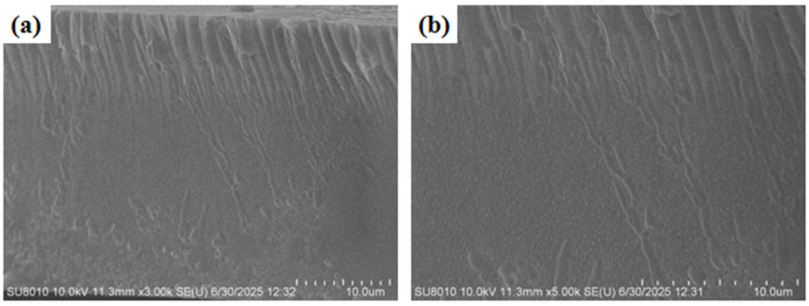

Figure 5. High-resolution cross-section SEM images of PFSA-25 membrane at different magnifications. (**a**) ×3000 magnification SEM cross-sectional view; (**b**) ×5000 magnification SEM cross-sectional view.

3.2. FT-IR Spectra

The characteristic peaks and functional groups of the PFSA membranes were characterized by FT-IR spectra. As shown in the FT-IR spectra of Figure 6, PFSA membranes with various thicknesses have approximately the same infrared spectrum shape. The figure shows a slight fluctuation in the curve at 3456 cm^{-1}, which is attributed to the O-H stretching vibration generated by physical water absorption [32]. For Nafion membranes, the fluctuation is not obvious, which implies a relatively low water uptake (WU) compared to Dongyue PFSA series membranes. The spectrum of the PFSA-55 membrane in the figure has the highest vibration amplitude at this point, corresponding to the membrane having the highest moisture content and WU [33,34]. The band at 1630 cm^{-1} corresponds to the O-H bending vibration of free water molecules, and the characteristic peaks of sulfonic acid groups can be observed at 1051.3 cm^{-1}, which belong to the symmetric stretching vibration band of S=O and the asymmetric stretching vibration band of S=O, respectively. The peaks at 1204.4 and 1140.6 cm^{-1} are attributed to the asymmetric stretching and symmetric stretching of C-F, respectively. Additionally, the two peaks at 984.3 and 966.1 cm^{-1} are attributed to C-O bonds. The band at 632 cm^{-1} is attributed to the stretching of the C-S group [31,35,36]. The shoulder peak near 1319.5 cm^{-1} comes from the C-C bond [37,38].

The chemical structures of Nafion and Dongyue PFSA are shown in Figure 7. The chemical structures of Dongyue PFSA and Nafion long side chain perfluorosulfonic acid resin are similar, except that the copolymer segment ratio is slightly different. The x value of Nafion is about 6.6 [39]. As can be seen from Figure 6, the characteristic peak of the Dongyue PFSA membrane at 1319 cm^{-1} is slightly lower than that of the Nafion membrane. This characteristic peak corresponds to the vibration absorption peak of the C-C bond. It can be inferred that the x value in the chemical structure of Dongyue PFSA resin is smaller than that of Nafion.

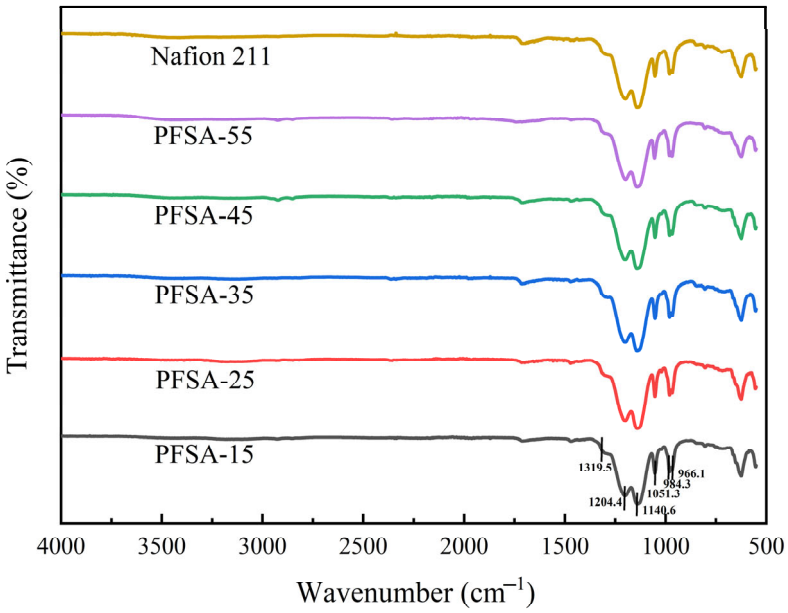

Figure 6. FTIR spectra of Nafion 211 and PFSA membranes with different thicknesses.

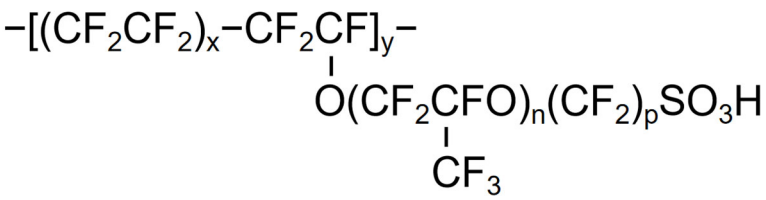

Figure 7. Chemical structures of Nafion 211 and Dongyue PFSA resin.

3.3. Physicochemical Properties

The WU and SR of the PEM affect the output performance of the membrane in PEMFC applications. The high water content and WU value in the PEMs enable the membrane with high proton conductivity and low internal resistance. Moreover, it also affects the microstructure and mechanical properties of the polymer. PEMFC pursues current density and higher power, and the PFSA membrane needs to be fully hydrated to have a higher proton conductivity [40]. Therefore, appropriate WU in the membrane is crucial to improving the output performance of fuel cells. The SR reflects the dimensional stability of the PEM, which can cause dilution of protons if the SR is extremely high, thereby reducing proton conductivity. Meanwhile, it can also cause deformation of the MEA and excessive local stress on the PEM, resulting in damage to the PEM and MEA. Therefore, it is necessary to strike a good balance between WU and SR [41]. The IEC value is a measure of the relative concentration of acid groups within a PEM, and an increase in the IEC value means an upward trend in the density of sulfonic acid groups for the PFSA membranes.

Table 1 lists the physical and chemical properties of all PFSA membrane samples used in this work. The WU and thickness SR of PFSA membranes with different thicknesses gradually rise with increasing thickness, which is caused by the increase in sulfonic acid groups in the membrane with expanding thickness. The values are significantly higher than those of the Nafion 211 membrane, suggesting that PFSA series membranes may have better proton conductivity. Based on the data in the table, it can be seen that the PEM exhibits different SR in the thickness direction and the plane direction, indicating that there are anisotropic differences in the spatial structure of the membrane [13]. The SR of PFSA membranes in the length direction does not exhibit an obvious trend of varying with thickness, but is much smaller than the thickness SR. It should be noted that excessively

high SR may lead to low proton conductivity of the PFSA series membrane. The IEC of PFSA membranes with different thicknesses is basically the same, all surpassing that of the Nafion 211 membrane, providing a basis for its higher proton conductivity. Subsequently, the proton conductivity of various Dongyue PFSA membrane samples was measured at 80 °C and 100% RH. It was found that except for PFSA-15, the proton conductivity declined with the expansion of membrane thickness, and all were higher than that of Nafion 211 (0.155 S·cm^{-1}). This result is basically consistent with the proton conductivity results of Nafion 211 in the literature [13]. Hence, the higher SR of Dongyue PFSA series membranes compared to commercial Nafion 211 may be caused by the differences between the preparation method and annealing temperature.

Table 1. Physical and chemical properties of Nafion 211 and PFSA series membranes with different thicknesses.

Samples	Thickness (μm)	WU (%)	Length SR (%)	Thickness SR (%)	IEC (mmol g^{-1})	Proton Conductivity at 80 °C (S cm^{-1})
PFSA-15	15 ± 2	28.57 ± 0.12	14.08 ± 0.21	23.53 ± 2.95	1.016 ± 0.005	0.326
PFSA-25	25 ± 2	29.03 ± 0.13	18.55 ± 0.08	27.59 ± 1.73	1.006 ± 0.003	0.371
PFSA-35	35 ± 2	29.17 ± 0.10	13.65 ± 0.07	30.56 ± 1.40	1.021 ± 0.003	0.311
PFSA-45	45 ± 2	30.00 ± 0.08	11.69 ± 0.17	38.78 ± 1.05	1.022 ± 0.001	0.204
PFSA-55	55 ± 2	32.03 ± 0.11	16.36 ± 0.09	40.35 ± 1.25	1.013 ± 0.004	0.190
Nafion 211	25	11.19 ± 0.09	3.35 ± 0.25	16.00 ± 2.00	0.813 ± 0.007	0.155

3.4. Mechanical Properties Test Results

Figure 8 shows the stress–strain curves of Dongyue PFSA series membranes with different thicknesses and commercial Nafion 211 as PEMs. Table 2 lists the tensile strength (MPa), elongation at break (%), maximum force (N), and fracture force (N) of all membranes. The maximum tensile force and breaking force of the PFSA series membrane samples increase with increasing thickness. Tensile strength exhibits a positive correlation with membrane thickness, but the overall difference is small. The elongation at break does not show an obvious trend of change with increasing thickness.

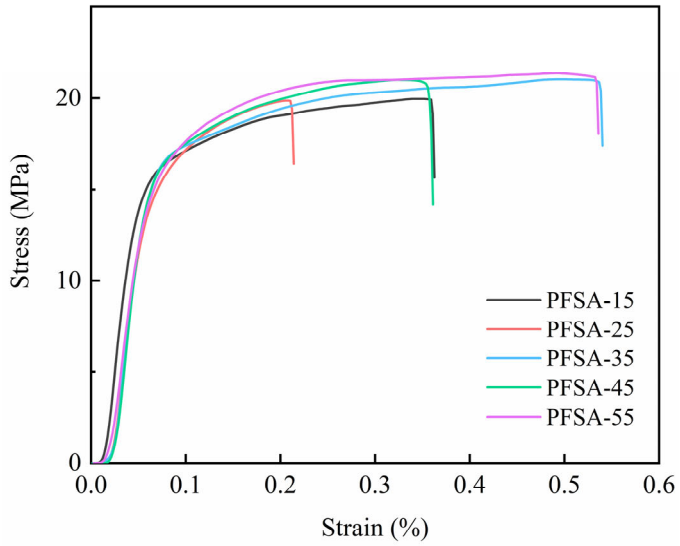

Figure 8. Stress–strain curves of PFSA membranes with different thicknesses.

Table 2. Mechanical properties of recast Nafion and Dongue PFSA membranes with different thicknesses.

Samples	Tensile Strength (MPa)	Elongation Percentage (%)	Maximum Force (N)	Breaking Force (N)
PFSA-15	19.96 ± 0.19	36.26 ± 0.80	7.19 ± 0.05	5.64 ± 0.13
PFSA-25	19.69 ± 0.17	21.40 ± 0.85	9.78 ± 0.01	8.08 ± 0.10
PFSA-35	21.03 ± 0.14	54.02 ± 0.88	14.72 ± 0.02	12.16 ± 0.07
PFSA-45	21.00 ± 0.15	36.11 ± 0.90	18.90 ± 0.04	12.75 ± 0.12
PFSA-55	21.36 ± 0.16	53.59 ± 1.05	23.50 ± 0.03	19.83 ± 0.11
Recast Nafion 50 μm	9.6 ± 0.2 [42]	41 ± 1 [42]	--	--

E.Y. Safronova et al. [42] investigated the mechanical properties of Nafion membranes with a thickness of 50 μm that were recast by dissolving and recasting in a water–alcohol solution. They found that the hydrophilic functional groups of Nafion were released on the surface of the spheres in the water–alcohol solution, and the polymers were easily aggregated, resulting in a decrease in their elongation at break (about 41%) to one-fifth of the commercial Nafion 212 membrane with a thickness of 50 μm. Moreover, there was a decrease in tensile strength to one-third of the commercial Nafion 212 membrane, about 9.6 MPa, which is much smaller than the PFSA series membrane. Therefore, the mechanical strength of Dongyue PFSA series membranes is superior to that of the water-alcohol solution recast Nafion membranes. If the same preparation method is used as commercial Nafion membranes, the mechanical properties of Dongyue PFSA series membranes will be significantly better.

3.5. Thermogravimetric Analysis (TGA) Test Results

The TGA curves of Dongyue PFSA membrane samples with different thicknesses all showed the same trend, as shown in Figure 9. The TGA curve shows three typical weight loss events. When the temperature is below 300 °C, the evaporation of water in the membrane sample causes a slight weight loss. At 300~400 °C, the PFSA side chain begins to decompose and the weight of the membrane sample begins to drop rapidly. The decomposition of the main chain of Dongyue PFSA membranes occurs at 420~500 °C, beyond which the membrane sample has been completely decomposed. Within the operating temperature range of PEMFC (60–90 °C), there is only a slight loss in the quality of the PFSA membrane, demonstrating high thermal stability.

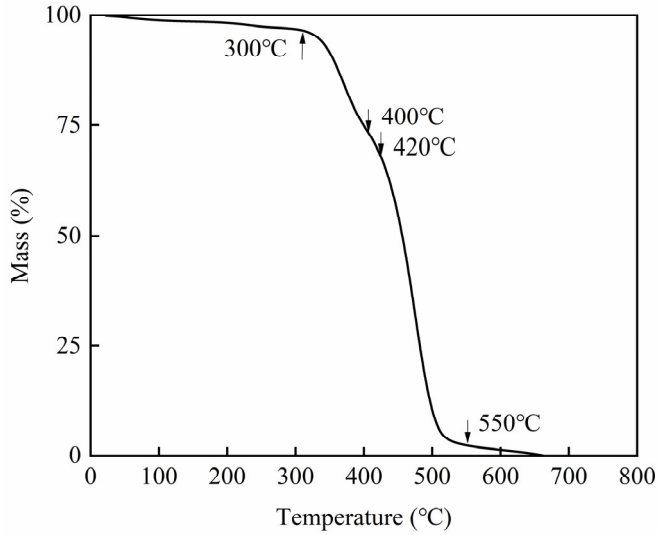

Figure 9. TGA curve of PFSA membrane.

3.6. Proton Conductivity Test Results

Figure 10 describes the comparison of the proton conductivity of the prepared Dongyue PFSA membranes with different thicknesses and Nafion 211 at different temperatures (50~90 °C) and 100% RH. The proton conductivity of all PFSA membranes shows an increasing trend with increasing temperature. Among them, PFSA-25 demonstrates the highest proton conductivity, reaching 0.387 S cm^{-1} at 90 °C, followed by PFSA-15 and PFSA-35. The proton conductivity of PFSA membranes with different thicknesses, prepared using Dongyue PFSA resins, is significantly higher than that of the commercial Nafion 211 membrane at various temperatures.

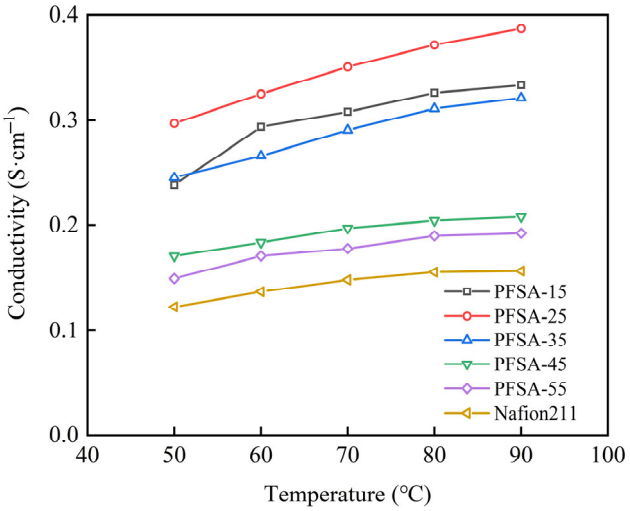

Figure 10. Proton conductivity of Nafion 211 and Dongyue PFSA membranes with different thicknesses as function of temperature.

3.7. Oxidation Stability

Figure 11 illustrates the changes in weight and proton conductivity of the PEMs before and after immersion in the Fenton solution, which can be considered the conditions for stimulating the accelerated oxidation experiment. After immersion, the mass loss of Dongyue PFSA series membranes is higher than that of Nafion 211. Among them, PFSA-15 experiences a maximum loss of 8%, which is slightly higher than that of Nafion 211 (1%). Moreover, after oxidation drying, Dongyue PFSA membranes become more brittle and prone to breakage. However, the loss rate of proton conductivity in PFSA-15, PFSA-25, and PFSA-35 is lower than that in Nafion 211, indicating a stronger ability to maintain proton conductivity. As shown in Figure 12, after oxidation, the proton conductivity of Nafion 211 decreased from 0.122 to 0.052 S·cm^{-1}, while that of the PFSA series membranes decreased to 0.080, 0.081, 0.113, 0.054, and 0.091 S·cm^{-1}, respectively, all of which were greater than that of the Nafion 211 membrane. However, due to the poor proton conductivity maintenance ability of PFSA-45 and PFSA-55, their proton conductivity may be lower than that of Nafion 211 with prolonged oxidation time.

The FT-IR image of the membranes after the Fenton oxidation experiment is shown in Figure 13. From the figure, it can be seen that all membranes exhibit a clear small absorption peak at 1465 cm^{-1}. This characteristic peak is attributed to the S=O in SO_2F or SO_2-O-SO_2, indicating that under the attack of HO and HOO radicals, sulfonic acid groups are converted to SO_2F or SO_2-O-SO_2 [37]. However, the characteristic peak intensity of PFSA-15 at this location is minimal, which may be due to the further decomposition of sulfonic acid groups into soluble SO_4^{2-} in water.

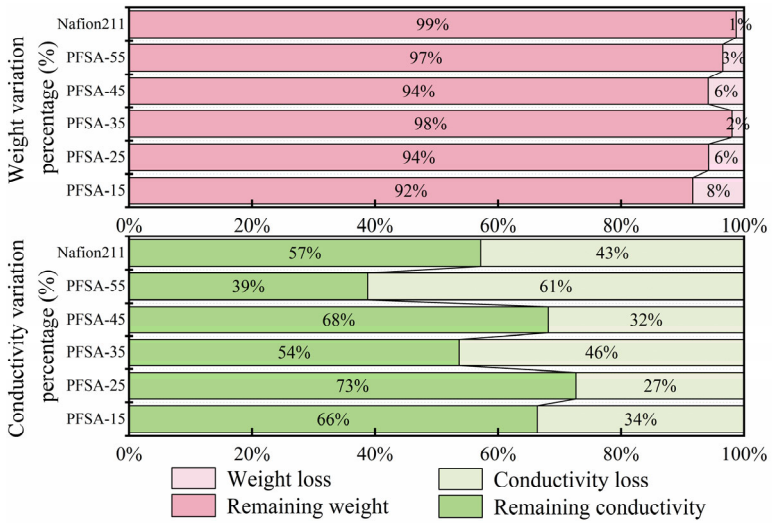

Figure 11. Variations in weight and proton conductivity of Nafion 211 and Dongyue PFSA membranes with different thicknesses before and after accelerated oxidation experiment.

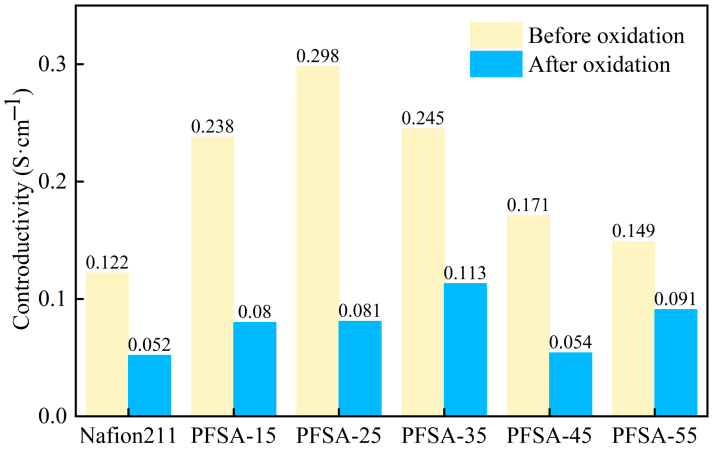

Figure 12. Proton conductivity of Nafion 211 and PFSA membranes with different thicknesses before and after accelerated oxidation experiment.

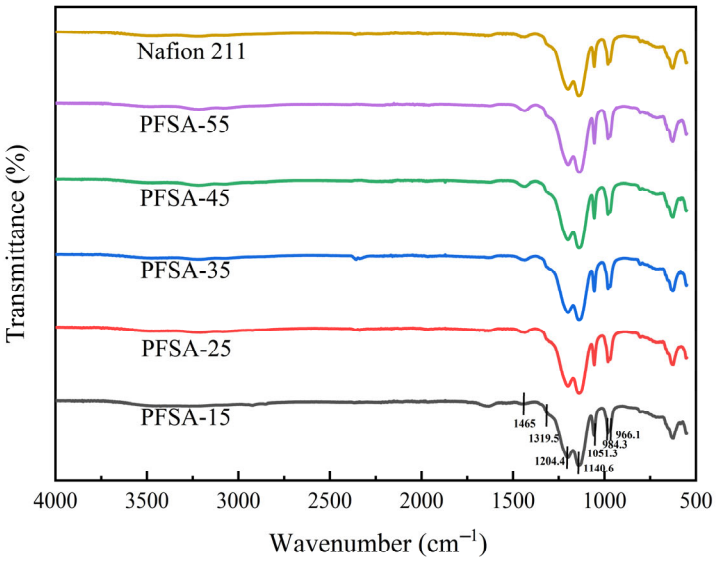

Figure 13. FT-IR spectra of Nafion 211 and PFSA membranes with different thicknesses before and after accelerated oxidation experiment.

3.8. PEMFC SINGLE Cell Performance

Dongyue PFSA series membranes with different thicknesses and Nafion 211 were assembled into a PEMFC single-cell for testing. Figure 14 shows the polarization curves of a PEMFC single-cell assembled with PFSA-15, PFSA-25, PFSA-35, PFSA-45, PFSA-55, and Nafion 211 membranes. Among them, the maximum power density of the PEMFC single-cell assembled with PFSA-25, PFSA-35, PFSA-45, and PFSA-15 is all higher than that of Nafion 211, reaching 851.76, 833.56, 688.62, and 659.92 mW·cm^{-2}, respectively, while the maximum power density of that assembled with Nafion 211 is 635.99 mW·cm^{-2} at 80 °C, 100% RH, and H_2/Air conditions, which is basically consistent with the results reported in the literature. Yazili et al. [43] tested the battery power density of Nafion 211 at a slightly higher temperature (84 °C), 85% RH, H_2/Air conditions, and found that its maximum power density was about 700 mW·cm^{-2}. The PFSA series membranes basically show a trend of promoting maximum power density of the PEMFC single-cell with increasing thickness, which is consistent with the theoretical basis that the thicker the PEM, the greater the internal resistance, leading to a decrease in PEMFC efficiency. However, the maximum power density of a PEMFC single-cell assembled with PFSA-15 is relatively small, which may be due to the low WU, low proton conductivity, and greater contact resistance of PFSA-15.

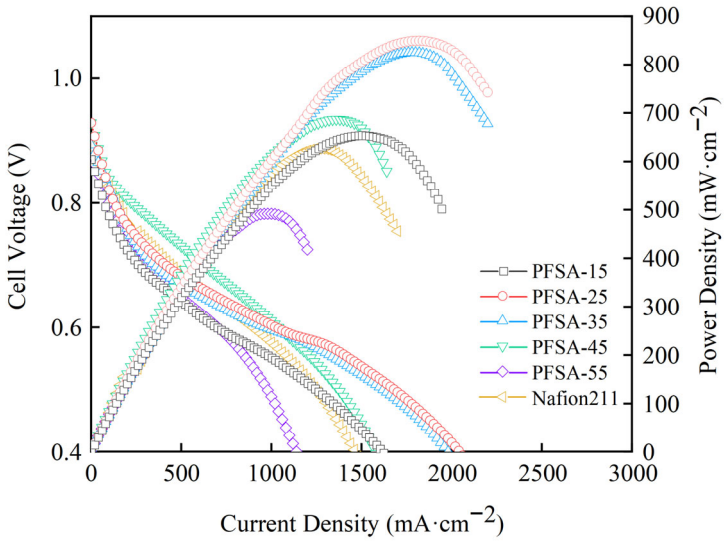

Figure 14. Polarization curves of PEMFC single-cell assembled with Nafion 211 and Dongyue PFSA series membranes.

According to the voltage variation curve in the figure, in the low current density range (activation polarization zone), the activation energy barrier of the reaction causes the reaction rate on the catalyst surface to be limited at the very beginning of PEMFC start-up. The voltage drop is related to the activity of the catalyst. Except for PFSA-45, the voltage drop of Dongyue PFSA series membranes is higher than that of Nafion 211, which may be due to the catalyst layer being too thick or poor interface contact with the catalyst layer. In the medium current density range (ohmic polarization region), the voltage and current density decrease approximately linearly. At this time, the voltage drop is mainly dominated by the internal ohmic resistance of the PEMFC single-cell. The voltage drop at this time can be arranged in the order of PFSA-25 < PFSA-35 < PFSA-15 < Nafion < PFSA-45 < PFSA-55, indicating that PFSA-25 has the best proton conductivity and the lowest contact resistance. In the high current density range (concentration polarization region), the reactant transfer rate cannot meet the high current demand, resulting in an increase in the concentration gradient on the electrode

surface, which causes the voltage to drop sharply. At this time, the voltage drop is arranged in the following order: PFSA-15 < PFSA-25 < PFSA-35 < Nafion < PFSA-45 < PFSA-55. In this region, PFSA-25 still performs more stably and has better performance.

As shown in Figure 15, the PEMFC single-cell assembled with GORE-SELECT® 8 μm PEM demonstrated excellent output performance in the polarization curve test, with a maximum power density of 1047 mW·cm^{-2}. Although this value is 1.23 and 1.26 times higher than that of PFSA-25 and PFSA-35 membranes, it should be noted as well that the thickness of PFSA-25 and PFSA-35 membranes is approximately 3.13 and 4.38 times that of GORE-SELECT® 8 μm membranes. Therefore, by comprehensively considering the raw material cost, preparation cost, and output performance, the PFSA series membranes still demonstrate a higher cost-effectiveness advantage.

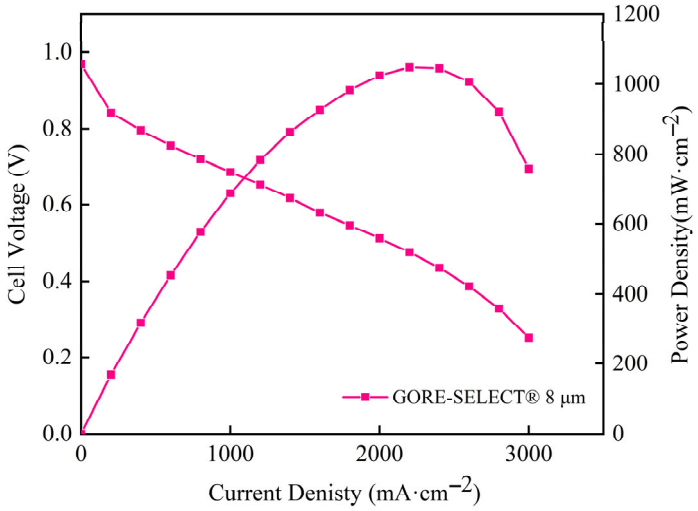

Figure 15. Polarization curve of PEMFC single-cell with GORE-SELECT® 8 μm membrane.

4. Conclusions

In this work, a series of Dongyue PFSA PEMs with different thicknesses was prepared and successfully employed in PEMFCs. The ion exchange capacity (IEC), water uptake (WU), and thickness swelling ratio (SR) of the Dongyue PFSA membranes were higher than those of Nafion 211 membranes. In terms of mechanical strength, the Dongyue PFSA series membranes demonstrate slightly better performance than the recast Nafion membranes. The tensile strengths of PFSA-25 and PFSA-35 were 19.8591 and 21.0326 MPa, respectively. If the same preparation process as Nafion or other better preparation processes were used, their mechanical properties would be further improved. However, in the Fenton accelerated oxidation experiment, the weight loss of the Dongyue PFSA membrane exceeded that of the commercial Nafion 211 membrane, and there is still room for improvement. In PEMFC single-cell tests, the maximum power density of PEMFC single-cells with PEM thicknesses of 15 μm, 25 μm, 35, and 45 μm are all higher than that of Nafion 211. The maximum power densities observed for the PEMFC single-cell assembled with Dongyue PFSA series membranes 25 and 35 μm are 851.76 and 833.56 mW·cm^{-2}, respectively, which are much higher than the 635.99 mW·cm^{-2} of Nafion 211, demonstrating an increase of 34 and 31%.

By comparing the physical and chemical properties of Dongyue PFSA PEMs with different thicknesses, it was found that 25 μm is the optimal membrane thickness for PEMFC applications. The investigations have confirmed that the developed PFSA membranes have the commercial potential to replace Nafion, and it is recommended to further promote its mechanical properties and antioxidant capacity through strategies such as composite reinforcement and optimized preparation process.

Author Contributions: Conceptualization, G.M. and C.S.; methodology, G.M. and C.S.; formal analysis, G.M., X.L. and C.S.; investigation, M.L. and G.M.; resources, M.L. and C.S.; data curation, G.M. and X.L.; writing—original draft preparation, G.M. and X.L.; writing—review and editing, G.M., S.A.G., I.T. and C.S.; visualization, G.M., J.S., C.Y. and X.L.; supervision, C.S.; funding acquisition, C.S. All authors have read and agreed to the published version of the manuscript.

Funding: This research was funded by the 2023 Youth Talent Introduction Scientific Research Startup Fee (Grant No. AUGA2160100623) and 2023 Support Funds for Talent Introduction in Heilongjiang Province (Grant No. AUGA2160501723) provided by the Harbin Institute of Technology, China.

Data Availability Statement: The original contributions presented in the study are included in the article; further inquiries can be directed to the corresponding author.

Acknowledgments: We would like to thank Yanbin Shao from the School of Chemistry and Chemical Engineering of Harbin Institute of Technology for providing the scanning electron microscope equipment for the experiment.

Conflicts of Interest: The authors declare no conflicts of interest.

Abbreviations

The following abbreviations are used in this manuscript:

PFSA	Perfluorosulfonic acid
PEMFC	Proton exchange membrane full cell
PEM	Proton exchange membrane
IEC	Ion exchange capacity
DMF	N, N-Dimethylformamide
SEM	Scanning electron microscopy
FT-IR	Fourier transform infrared
WU	Water uptake
SR	Swelling ration
MEA	Membrane electrode assembly
EIS	Electrochemical impedance spectroscopy
TGA	Thermogravimetric analysis
GDL	Gas diffusion layer
GDE	Gas diffusion electrode

References

1. Shafiee, S.; Topal, E. When will fossil fuel reserves be diminished? *Energy Policy* **2009**, *37*, 181–189. [CrossRef]
2. Bach, W. Fossil fuel resources and their impacts on environment and climate. *Int. J. Hydrogen Energy* **1981**, *6*, 185–201. [CrossRef]
3. Li, X.; Ye, T.; Meng, X.; He, D.; Li, L.; Song, K.; Jiang, J.; Sun, C. Advances in the Application of Sulfonated Poly(Ether Ether Ketone) (SPEEK) and Its Organic Composite Membranes for Proton Exchange Membrane Fuel Cells (PEMFCs). *Polymers* **2024**, *16*, 2840. [CrossRef] [PubMed]
4. Peighambardoust, S.J.; Rowshanzamir, R.; Amjadi, R. Review of the proton exchange membranes for fuel cell applications. *Int. J. Hydrogen Energy* **2010**, *35*, 9349–9384. [CrossRef]
5. Wu, C.; Burke, T. Intelligent computer aided optimization on specific power of an OTEC Rankine power plant. *Appl. Therm. Eng.* **1998**, *18*, 295–300. [CrossRef]
6. Ajanovic, A.; Haas, R. Economic prospects and policy framework for hydrogen as fuel in the transport sector. *Energy Policy* **2018**, *123*, 280–288. [CrossRef]
7. Hames, Y.; Kaya, K.; Baltacioglu, E.; Turksoy, A. Analysis of the control strategies for fuel saving in the hydrogen fuel cell vehicles. *Int. J. Hydrogen Energy* **2018**, *43*, 10810–10821. [CrossRef]
8. Meng, X.; Mei, J.; Tang, X.; Jiang, J.; Sun, C.; Song, K. The degradation prediction of proton exchange membrane fuel cell performance based on a transformer model. *Energies* **2024**, *17*, 3050. [CrossRef]
9. Li, H.Y.; Liu, Y.L. Nafion-functionalized electrospun poly(vinylidene fluoride) (PVDF) nanofibers for high performance proton exchange membranes in fuel cells. *J. Mater. Chem. A* **2014**, *2*, 3783–3793. [CrossRef]

10. Devanathan, R. Recent developments in proton exchange membranes for fuel cells. *Energy Environ. Sci.* **2008**, *1*, 101–119. [CrossRef]
11. Park, J.; Oh, H.; Ha, T.; Lee, Y.I.; Min, K. A review of the gas diffusion layer in proton exchange membrane fuel cells: Durability and degradation. *Appl. Energy* **2015**, *155*, 866–880. [CrossRef]
12. Farooqui, U.R.; Ahmad, A.L.; Hamid, N.A. Graphene oxide: A promising membrane material for fuel cells. *Renew. Sustain. Energy Rev.* **2018**, *82 Pt 1*, 714–733. [CrossRef]
13. Peron, J.; Mani, A.; Zhao, X.; Edwards, D.; Adachi, M.; Soboleva, T.; Shi, Z.; Xie, Z.; Navessin, T. Steven Holdcroft Properties of Nafion NR-211 membranes for PEMFCs. *J. Membr. Sci.* **2010**, *356*, 44–51. [CrossRef]
14. Şengül, E.; Erdener, H.; Akay, R.G.; Yücel, H.; Baç, N.; Eroğlu, İ. Effects of sulfonated polyether-etherketone (SPEEK) and composite membranes on the proton exchange membrane fuel cell (PEMFC) performance. *Int. J. Hydrogen Energy* **2009**, *34*, 4645–4652. [CrossRef]
15. Teixeira, F.C.; Teixeira, A.P.; Rangel, C.M. New Modified SPEEK-Based Proton Exchange Membranes. *Polymers* **2025**, *17*, 1646. [CrossRef] [PubMed]
16. Sun, C.; Negro, E.; Vezzù, K.; Pagot, G.; Cavinato, G.; Nale, A.; Bang, Y.H.; Di Noto, V. Hybrid inorganic-organic proton-conducting membranes based on SPEEK doped with WO_3 nanoparticles for application in vanadium redox flow batteries. *Electrochim. Acta* **2019**, *309*, 311–325. [CrossRef]
17. Yu, J.-r.; Yi, B.-l.; Han, M. Influence of the Nation membrane thickness on the performance of proton exchange membrane fuel cells. *Chin. J. Power Sources* **2001**, *25*, 384–386.
18. Dimitrova, P.; Friedrich, K.A.; Vogt, B.; Stimming, U. Transport properties of ionomer composite membranes for direct methanol fuel cells. *J. Electroanal. Chem.* **2002**, *532*, 75–83. [CrossRef]
19. Silva, R.; De Francesco, M.; Pozio, A. Tangential and normal conductivities of Nafion® membranes used in polymer electrolyte fuel cells. *J. Power Sources* **2004**, *134*, 18–26. [CrossRef]
20. Tsampas, M.N.; Pikos, A.; Brosda, S.; Katsaounis, A.; Vayenas, C.G. The effect of membrane thickness on the conductivity of Nafion. *Electrochim. Acta* **2006**, *51*, 2743–2755. [CrossRef]
21. Büchi, F.N.; Scherer, G.G. Investigation of the transversal water profile in Nafion membranes in polymer electrolyte fuel cells. *J. Electrochem. Soc.* **2001**, *148*, A183. [CrossRef]
22. Karimi, M.B.; Mohammadi, F.; Hooshyari, K. Recent approaches to improve Nafion performance for fuel cell applications: A review. *Int. J. Hydrogen Energy* **2019**, *44*, 28919–28938. [CrossRef]
23. Yin, C.; Li, J.; Zhou, Y.; Zhang, H.; Fang, P.; He, C. Phase separation and development of proton transport pathways in metal oxide nanoparticle/nafion composite membranes during water uptake. *J. Phys. Chem. C* **2018**, *122*, 9710–9717. [CrossRef]
24. Di Noto, V.; Boaretto, N.; Negro, E.; Stallworth, P.E.; Lavina, S.; Giffin, G.A.; Greenbaum, S.G. Inorganic–organic membranes based on Nafion, $[(ZrO_2)\cdot(HfO_2)_{0.25}]$ and $[(SiO_2)\cdot(HfO_2)_{0.28}]$ nanoparticles. Part II: Relaxations and conductivity mechanism. *Int. J. Hydrogen Energy* **2012**, *37*, 6215–6227. [CrossRef]
25. Vittadello, M.; Negro, E.; Lavina, S.; Pace, G.; Safari, A.; Noto, V.D. Vibrational studies and properties of hybrid inorganic−organic proton conducting membranes based on Nafion and hafnium oxide nanoparticles. *J. Phys. Chem. B* **2008**, *112*, 16590–16600. [CrossRef] [PubMed]
26. Vinothkannan, M.; Ramakrishnan, S.; Kim, A.R.; Lee, H.K.; Yoo, D.J. Ceria Stabilized by Titanium Carbide as a Sustainable Filler in the Nafion Matrix Improves the Mechanical Integrity, Electrochemical Durability, and Hydrogen Impermeability of Proton-Exchange Membrane Fuel Cells: Effects of the Filler Content. *ACS Appl. Mater. Interfaces* **2020**, *12*, 13. [CrossRef] [PubMed]
27. Sun, C.; Negro, E.; Nale, A.; Pagot, G.; Vezzù, K.; Zawodzinski, T.A.; Meda, L.; Gambaro, C.; Di Noto, V. An efficient barrier toward vanadium crossover in redox flow batteries: The bilayer [Nafion/$(WO_3)_x$] hybrid inorganic-organic membrane. *Electrochim. Acta* **2021**, *378*, 138133. [CrossRef]
28. Zhang, J.-H.; Guo, G.-B.; An, S.-L.; Hao, Y.; Zhang, D.; Yan, K.-B. Synthesis and properties of proton exchange membranes via single-step grafting PSBMA onto PVDF modified by TMAH. *Acta Phys.-Chim. Sin.* **2015**, *31*, 1905–1913. [CrossRef]
29. Dai, W.; Shen, Y.; Li, Z.; Yu, L.; Xi, J.; Qiu, X. SPEEK/Graphene oxide nanocomposite membranes with superior cyclability for highly efficient vanadium redox flow battery. *J. Mater. Chem. A* **2014**, *2*, 12423–12432. [CrossRef]
30. Meng, X.; Sun, C.; Mei, J.; Tang, X.; Hasanien, H.M.; Jiang, J.; Fan, F.; Song, K. Fuel cell life prediction considering the recovery phenomenon of reversible voltage loss. *J. Power Sources* **2025**, *625*, 235634. [CrossRef]
31. Sigwadi, R.; Dhlamini, M.; Mokrani, T.; Ṇemavhola, F.; Nonjola, P.; Msomi, P. The proton conductivity and mechanical properties of Nafion®/ZrP nanocomposite membrane. *Heliyon* **2019**, *5*, e02240. [CrossRef] [PubMed]
32. Li, Y.; Zhang, J.; Han, W.; Liu, B.; Zhai, M.; Li, N.; Wang, Z.; Zhao, J. Multifunctional Laser-Induced Graphene-Based Microfluidic Chip for High-Performance Oocyte Cryopreservation with Low Concentration of Cryoprotectants. *Adv. Healthc. Mater.* **2024**, *13*, 2400981. [CrossRef] [PubMed]

33. Yang, H.N.; Lee, D.C.; Park, S.H.; Kim, W.J. Preparation of Nafion/various Pt-containing SiO_2 composite membranes sulfonated via different sources of sulfonic group and their application in self-humidifying PEMFC—ScienceDirect. *J. Membr. Sci.* **2013**, *443*, 210–218. [CrossRef]
34. Arico', A.S.; Baglio, V.; Blasi, A.D.; Antonucci, V. FTIR spectroscopic investigation of inorganic fillers for composite DMFC membranes. *Electrochem. Commun.* **2003**, *5*, 862–866. [CrossRef]
35. Di Noto, V.; Gliubizzi, R.; Negro, E.; Pace, G. Effect of SiO_2 on relaxation phenomena and mechanism of ion conductivity of [Nafion/$(SiO_2)_x$] composite membranes. *J. Phys. Chem. B* **2006**, *110*, 24972–24986. [CrossRef] [PubMed]
36. Laporta, M.; Pegoraro, M.; Zanderighi, L. Perfluorosulfonated membrane (Nafion): FT-IR study of the state of water with increasing humidity. *Phys. Chem. Chem. Phys.* **1999**, *1*, 4619–4628. [CrossRef]
37. Kinumoto, T.; Inaba, M.; Nakayama, Y.; Ogata, K.; Umebayashi, R.; Tasaka, A.; Iriyama, Y.; Abe, T.; Ogumi, Z. Durability of perfluorinated ionomer membrane against hydrogen peroxide. *J. Power Sources* **2006**, *158*, 1222–1228. [CrossRef]
38. Gruger, A.; Régis, A.; Schmatko, T.; Colomban, P. Nanostructure of Nafion® membranes at different states of hydration: An IR and Raman study. *Vib. Spectrosc.* **2001**, *26*, 215–225. [CrossRef]
39. Shin, S.-H.; Nur, P.J.; Kodir, A.; Kwak, D.-H.; Lee, H.; Shin, D.; Bae, B. Improving the mechanical durability of short-side-chain perfluorinated polymer electrolyte membranes by annealing and physical reinforcement. *ACS Omega* **2019**, *4*, 19153–19163. [CrossRef] [PubMed]
40. Yan, S.; Yang, M.; Sun, C.; Xu, S. Liquid water characteristics in the compressed gradient porosity gas diffusion layer of proton exchange membrane fuel cells using the Lattice Boltzmann Method. *Energies* **2023**, *16*, 6010. [CrossRef]
41. Wang, G.; Kang, J.; Yang, S.; Lu, M.; Wei, H. Influence of structure construction on water uptake, swelling, and oxidation stability of proton exchange membranes. *Int. J. Hydrogen Energy* **2024**, *50*, 279–311. [CrossRef]
42. Safronova, E.Y.; Voropaeva, D.Y.; Lysova, A.A.; Korchagin, O.V.; Bogdanovskaya, V.A.; Yaroslavtsev, A.B. On the properties of Nafion membranes recast from dispersion in N-Methyl-2-Pyrrolidone. *Polymers* **2022**, *14*, 5275. [CrossRef] [PubMed]
43. Yazili, D.; Marini, E.; Saatkamp, T.; Münchinger, A.; de Wild, T.; Gubler, L.; Titvinidze, G.; Schuster, M.; Schare, C.; Jörissen, L. Sulfonated Poly (Phenylene sulfone) blend membranes finding their way into proton exchange membrane fuel cells. *J. Power Sources* **2023**, *563*, 232791. [CrossRef]